Supplementary Information

Phase-selective cation-exchange chemistry in sulfide nanowire systems

Dandan Zhang[†,§], Andrew B. Wong[†,§], Yi Yu[†,§], Sarah Brittman[†,§], Jianwei Sun[†,§], Anthony Fu[†,§], Brandon Beberwyck[‡,§,||], A. Paul Alivisatos[†,‡,§,||], Peidong Yang[*,†,‡,§,||]

[†]Department of Chemistry, University of California, Berkeley, CA 94720, United States

[‡]Department of Materials Science and Engineering, University of California, Berkeley, CA 94720, United States

[§]Materials Sciences Division, Lawrence Berkeley National Laboratory, Berkeley, CA 94720, United States

[||] Kavli Energy Nanoscience Institute, Berkeley, CA 94720, United States

Experimental details:

Synthesis of CdS nanowires: All chemicals were used as received without further purification. CdS nanowires were synthesized via a reported solvothermal approach with slight modification[1,2]. Briefly, 0.2 g cadmium diethyldithiocarbamate ($[Cd\text{-}(DDTC)_2]_2$) (96%, Gelest) was dissolved in 20 mL ethylenediamine (>99%, Sigma-Aldrich) and transferred to a Teflon-lined stainless steel autoclave. The autoclave was sealed and maintained at 200 °C for 15 hours, then allowed to cool to room temperature naturally. The yellowish precipitate of CdS nanowires was isolated by centrifugation at 6000 rpm for 3 mins and washed three times with methanol (certified ACS, Fisher Scientific). The CdS nanowires were stored in a nitrogen-filled glovebox.

Cation exchange of CdS nanowires: For the cation-exchange reaction tetrakis(acetonitrile)copper(I) hexafluorophosphate ($[MeCN]_4Cu^IPF_6$) (97%, Aldrich) was used as the source of Cu^+ cations, which is similar to previous work[3]. The reactions were always performed inside a nitrogen-filled glovebox at room temperature. In a typical reaction, 0.9 mg of as-synthesized CdS was redispersed in 9 mL anhydrous methanol (99.9%, Alfa Aesar) with brief sonication. $[MeCN]_4Cu^IPF_6$ was dissolved in 10 mL anhydrous methanol. After the addition of the Cu^+ solution, the yellow suspension of CdS nanowires immediately turned dark brown, indicating the initiation of the conversion from CdS to $Cu_{2-x}S$. Two independent reaction variables were systematically investigated in the study: the time of reaction, and the concentration of Cu^+ solution, which determined the $[Cu^+]/[Cd^{2+}]$ ratio. The nanowires were isolated at different reaction times, from 5 mins up to 200 hours, and the $[Cu^+]/[Cd^{2+}]$ ratio varied from 0.2:1 to 300:1. After the reaction, the nanowires were washed in methanol, followed by centrifugation at 6000 rpm for 5 mins and removal of the supernatant. Table S1 details the specific reaction conditions used to produce the CdS-$Cu_{2-x}S$ and $Cu_{2-x}S$ nanowires characterized in this work.

Charaterization: Powder X-ray diffraction (XRD) patterns of the obtained products were measured on a Bruker AXS D8 Advance diffractometer with a Co Kα source. The transmission

electron microscopy (TEM), high-resolution TEM (HRTEM) images and selected-area electron diffraction (SAED) patterns were taken with a FEI Tecnai TEM at an accelerating voltage of 200 kV. The energy-dispersive X-ray spectroscopy (EDS) elemental mapping images were recorded on a FEI Titan-X TEM at 80 kV. The scanning electron microscopy (SEM) images were taken with a JOEL field emission SEM at an accelerating voltage of 5 kV.

Table S1: Reaction conditions used to synthesize CdS-$Cu_{2-x}S$ nanowires and $Cu_{2-x}S$ nanowires by Cu^+ cation exchange of CdS nanowires

Sample	$[Cu^+]/[Cd^{2+}]$	Reaction time	TEM/XRD shown in Figure X
1	0.2	2 h	2
2	0.5	2 h	3a
3	1	2 h	3b
4	2	2 h	3c
5	10	2 h	3d, 4
7	10	10 min	S5
8	10	140 h	S5

Table S2. Crystal structure data of CdS[3] and different phases of $Cu_{2-x}S$[4,5]

	Composition	Crystal structure	Crystal structure for convenience
CdS	CdS	Hexagonal a_1 = 4.160 Å c_1 = 6.756 Å	
High-chalcocite	Cu_2S	Hexagonal a_2 = 3.95 Å c_2 = 6.75 Å	a=a c=c_h
Roxbyite	$Cu_{1.74-1.82}S$	Triclinic ($4Cu_{29}S_{16}$ *) a_3 = 13.409 Å b_3 = 13.405 Å c_3 = 15.485 Å α_1 = 90.022° β_1 = 90.021° γ_1 = 90.022°	orthorhombic a=13.409 Å =2c_h b=13.405 Å=2$\sqrt{3}a_h$ c=15.485 Å =4a_h
Djurleite	$Cu_{1.934-1.965}S$	Monoclinic ($8Cu_{31}S_{16}$) a_4 = 26.897 Å b_4 = 15.745 Å c_4 = 13.565 Å β_2 = 90.13°	orthorhombic a=26.897 Å =4c_h b=15.745 Å =4a_h c=13.565 Å=2$\sqrt{3}a_h$
Low-chalcocite	$Cu_{1.997-2}S$	Monoclinic ($48Cu_2S$) a_5 = 15.246 Å b_5 = 11.884 Å c_5 = 13.494 Å β_3 = 116.35°	Pseudo-orthorhombic a=11.92 Å =3a_h b=27.34 Å =4$\sqrt{3}a_h$ c=13.494 Å =2c_h

* indicates the unit cell composition

Table S3. Lattice parameters of the sulfur sublattice of CdS[3] and different phases of $Cu_{2-x}S$[4,5]

	a	c
CdS	4.160 Å	6.756 Å
Roxbyite	3.870 Å	6.705 Å
Djurleite	3.926 Å	6.724 Å
Low chalcocite	3.959 Å	6.747 Å

Table S4. Calculated lattice mismatch in between different species along a direction

CdS	Roxbyite	Djurleite	Low chalcocite	
0	6.97%	5.62%	4.83%	CdS
	0	1.42%	2.23%	Roxbyite
		0	0.84%	Djurleite
			0	Low chalcocite

Table S5. Calculated lattice mismatch in between different species along c direction

CdS	Roxbyite	Djurleite	Low chalcocite	
0	0.75%	0.47%	0.13%	CdS
	0	0.28%	0.62%	Roxbyite
		0	0.34%	Djurleite
			0	Low chalcocite

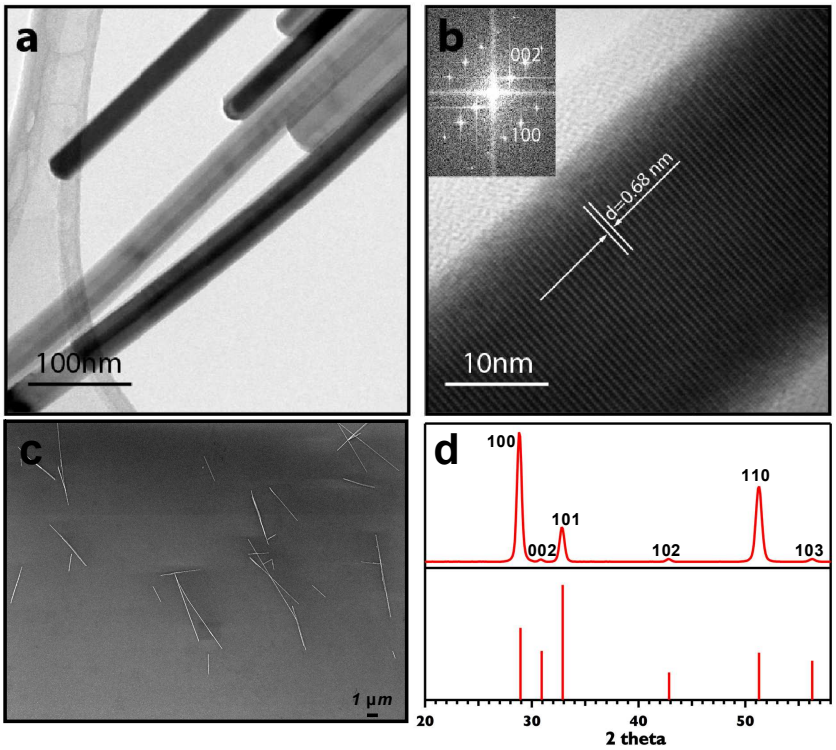

Figure S1. Structural characterization of CdS nanowires. (a) Representative TEM image of as-grown CdS nanowires. (b) High-resolution TEM image of an individual CdS nanowire, showing the single-crystalline structure. Inset: FFT image of the same wire, showing its <002> growth direction. (c) SEM image of the CdS nanowires spin-coated on a Si substrate with lengths up to 10 μm. (d) Experimental (top) and reference (bottom) XRD spectrum of CdS nanowires drop-cast onto a glass slide. The results show that the CdS nanowires grow in a preferential orientation along the c axis, hence the (002) peak is weakest, which is consistent with the growth direction shown in Figure S1b, since most of the wires are lying flat.

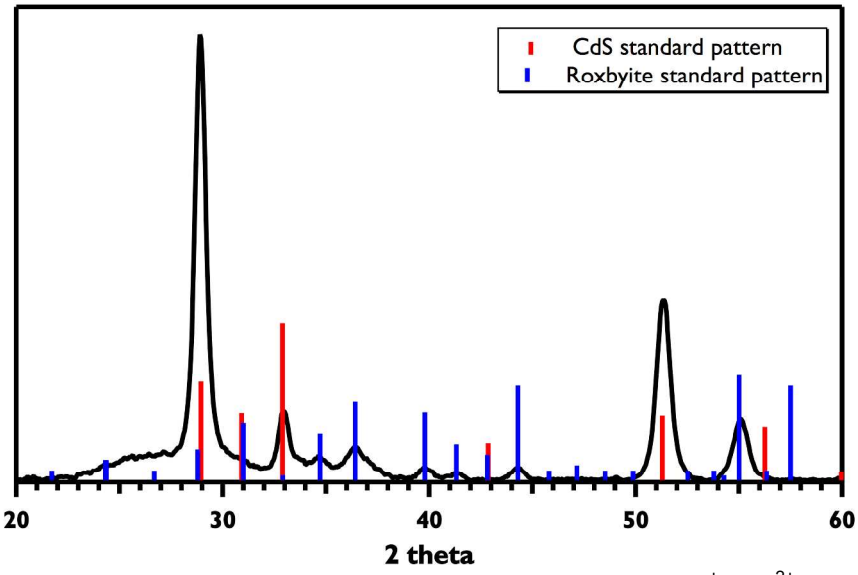

Figure S2. XRD patterns of the CdS-$Cu_{2-x}S$ core-shell nanowires with 1:1 $[Cu^{+}]/[Cd^{2+}]$ ratio and 2 h reaction.

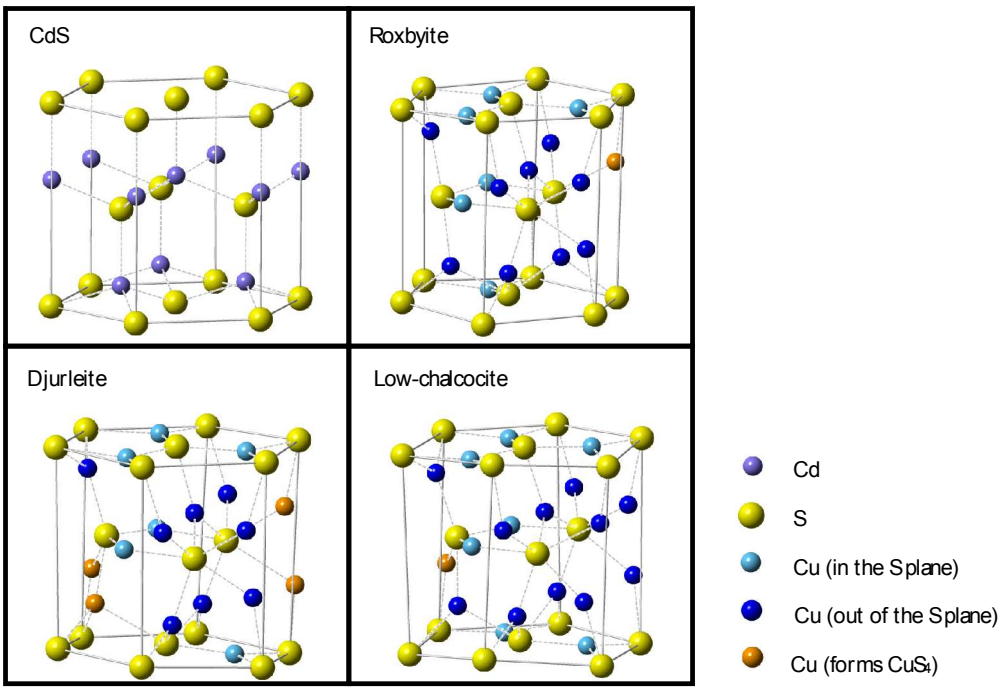

Figure S3. CdS unit cell and simplified crystal structures of roxbyite, djurleite and low-chalcocite, showing a similar S^{2-} sublattice.

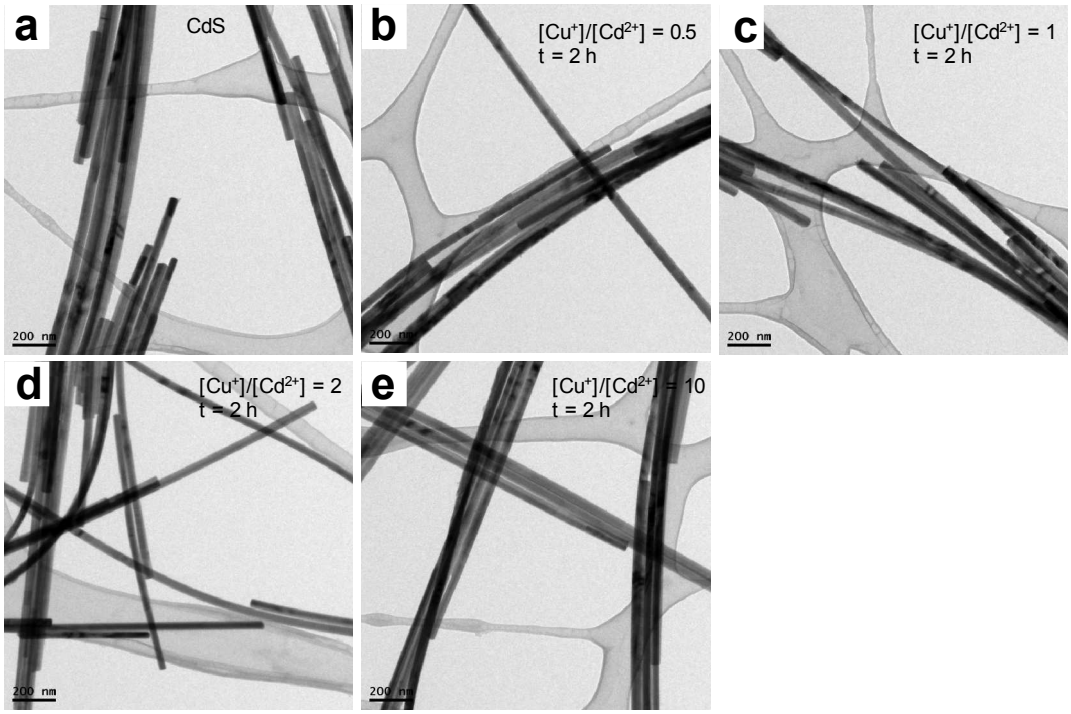

Figure S4. Low resolution TEM images of CdS, CdS-$Cu_{2-x}S$, and $Cu_{2-x}S$ nanowires, showing the morphology of the CdS nanowires is preserved after the cation-exchange reaction.

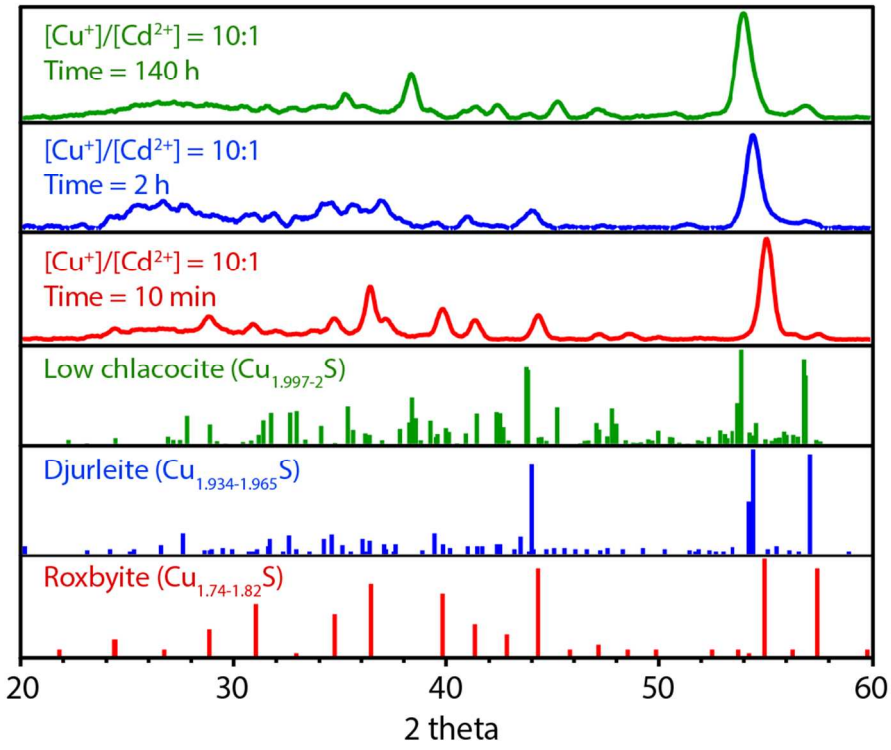

Figure S5. XRD patterns of the $Cu_{2-x}S$ nanowires obtained with different cation-exchange reaction times and same $[Cu^+]/[Cd^{2+}]$ ratio, showing that with longer reaction time, the resultant $Cu_{2-x}S$ nanowires evolve into more stoichometric phases. (upper three) Experimental spectrums of $Cu_{2-x}S$ nanowires prepared under different reaction conditions. (lower three) Standard patterns of low chalcocite, djurleite and roxbyite. The missing major peaks and the different intensity of the experimental spectra compared to the standard patterns are caused by the preferential orientation of the nanowires.

(1) Yan, P.; Xie, Y.; Qian, Y.; Liu, X. *Chem. Commun.* **1999**, 1293.
(2) Jen-La Plante, I.; Zeid, T. W.; Yang, P.; Mokari, T. *J. Mater. Chem.* **2010**, 20, 6612.
(3) Sadtler, B.; Demchenko, D. O.; Zheng, H.; Hughes, S. M.; Merkle, M. G.; Dahmen, U.; Wang, L.-W.; Alivisatos, A. P. *J. Am. Chem. Soc*. **2009**, *131*, 5285.
(4) Putnis, A. *Am. Mineral.* **1977**, *62*, 107.
(5) Mumme, W. G.; Gable, R. W.; Petricek, V. *Can. Mineral.* **2012**, 50, 423.